Computers in Biology and Medicine 112 (2019) 103359

Contents lists available at ScienceDirect

Computers in Biology and Medicine

journal homepage: www.elsevier.com/locate/compbiomed

Plug and play self-configurable IoT gateway node for telemonitoring of ECG

Aneesh M. Koya*, P.P. Deepthi

Department of Electronics and Communication Engineering, National Institute of Technology, Calicut, Kerala, India

ARTICLE INFO

Keywords:
Compressed sensing (CS)
Deterministic binary block diagonal (DBBD) matrix
Electrocardiogram (ECG) monitoring
Energy efficiency
Heterogeneous multi-processing (HMP)
Inter-pulse interval (IPI)
Wireless body area network (WBAN)

ABSTRACT

In the era of IoT and hyperconnection, an efficient electrocardiogram (ECG) telemonitoring system in wireless body area network (WBAN) demands an easy to use, self-configurable, secure, plug and play system with minimum hardware and computational complexities. The compression and quantization parameters required for an efficient representation of ECG signal will vary from patient to patient, from lead to lead, and from time to time. To this end, we propose a compressed sensing based WBAN with self-configurable gateway node (CS-SCGN) using deterministic binary block diagonal (DBBD) measurement matrix. The self-configurability is brought in through a low complex method for adaptive tuning of parameters with a careful choice of measurement matrix and data length. The redundant data transfer between sensor nodes and gateway node is avoided by addressing the diverse requirements in ECG remote health monitoring through three modes of configuration in the proposed system. A further reduction in communication and storage cost is achieved by optimizing the number of bits transmitted by sensor nodes by automatically tuning the compression ratio and quantization depth based on the dynamics of ECG signal. The self-configuration algorithm is designed to run at the gateway node in such a way as to optimize the power efficiency of sensor nodes without causing an extra power drain at the gateway node. Also, we investigate the feasibility of using smartphone as an IoT gateway node for performing primary processing to provide local utility before sending the received data to the remote server. The energy efficiency and real-time feasibility of the proposed algorithm are evaluated by implementing the gateway node on Odroid-XU4 board which runs on the same processor as in the latest smartphones. The experimental results indicate that our proposed self-configurable system at the gateway node makes the entire ECG telemonitoring system flexible, plug and play, patient independent and power-efficient.

1. Introduction

Nowadays, telemonitoring of physiological signals like electrocardiogram (ECG), photoplethysmogram (PPG), electroencephalogram (EEG), electromyogram (EMG), blood pressure level, etc. are becoming very crucial in the diagnosis and treatment of several diseases. The rapid advancement in Internet of Things (IoTs) paved the way for a technological revolution in healthcare industry [1–3]. Wireless body area network (WBAN) [4,5] systems play a significant role in the IoT based healthcare applications. In many countries, one of the leading causes of death is cardiovascular disease (CVD) [6]. Continuous monitoring of heart activities is essential to tackle the danger of CVD as well as to enhance the cardiovascular diagnosis [7–10]. This will result in massive amount of ECG data to be transmitted and stored [11–13]. Handling the transmission of this bulk data poses a great challenge on health care IoT with a tight constraint on energy consumption.

The morphology of ECG signal is governed by the action potentials generated from multitude of cardiac cells and their sequence of activation, resulting in a time-varying sparsity nature of the signal [14]. Other physiological factors such as differences in the heart position, size, and physical conditions contribute to the heterogeneity of ECG morphology among individuals. The cardiac dynamics [15] can be viewed as a spatial-temporal impression that reflects the temporal changes in the ECG signal. For such a signal, it is highly beneficial to have the compression and quantization parameters to be in tune with the signal dynamics.

WBAN sensor nodes are tiny battery powered devices with tight resource constraints. Due to the limited power available, the expensive wireless transmission of massive data from sensor nodes to the gateway node must take into account the variation in compression and quantization parameters for the efficient representation of ECG signal from time to time. The vendors either enforce the users to correctly configure the sensor nodes with the gateway node or provide sensor nodes with a commonly acceptable configuration setting. Need for intervention burdens the user in the former case whereas, the optimum configuration is less likely to be achieved in the latter case. Both the cases are not

* Corresponding author.
E-mail address: aneeshkoya@gmail.com (A.M. Koya).

https://doi.org/10.1016/j.compbiomed.2019.103359
Received 22 March 2019; Received in revised form 26 June 2019; Accepted 15 July 2019

favorable as the users are concerned, which ultimately increases the acceptance barrier. Hence the connectivity of ECG sensor nodes to the IoT network should be backed up by the plug and play functionality [16]. The design of an energy efficient plug and play sensor node remains an open challenge to the research community. The energy consumption of a sensor node is dominated by its transmission costs. So there is a high requisition to reduce the transmission costs without compromising the plug and play functionality.

Compressed sensing (CS) has been extensively used to facilitate the measurement process in WBAN [11,12,17,18]. CS [19–21] involves a simple linear encoding procedure which significantly reduces the compression complexity at the transmitter side. Authors in Ref. [17] have shown that CS increases the energy efficiency of the biosensing node compared to Nyquist sampling. Rate adaptivity in CS framework is attempted by various researchers in the recent literature. In Ref. [22], a rate adaptive CS scheme using change point method (CPM) is considered, in which the optimum compression rate is estimated by detecting the change in sparsity. The sensor node has to send additional cross-validation measurements to the gateway based on a given error bound. Their scheme involves CS recovery, CPM, and sparsity estimation at the gateway node. But CS recovery is computationally intensive and power hungry. In Ref. [23], the authors presented an end to end CS system using padded binary permuted block diagonal (BPBD) matrix in which the compression parameter is tuned by means of mirror padding of samples. Some limitations of the method are (i) padding of symmetric elements may significantly distort or alter the original signal, (ii) raw (uncompressed) sensor data is employed for tuning the parameter which will increase the transmission cost, and (iii) additional buffer is required. Both the above methods try to achieve adaptability through tuning a single parameter, i.e., compression parameter.

There are papers in the literature that addresses the adaptation of both compression and quantization parameters in CS framework. In Ref. [18], a configurable quantized CS architecture for WBAN is presented; but that algorithm cannot be used for real-time plug and play operation. It is running offline due to the time-consuming ℓ_1 -norm solver in the reconstruction stage. A dynamic knob design to configure the parameters in CS framework was provided in Ref. [24]. The design is based on a supervised learning algorithm which is computationally intensive and time-consuming. The parameter estimation is done using a lookup table module based on predefined templates.

With the ability to self-configure the sampling and quantization of sensor nodes, gateway nodes can help to save the battery power of sensor nodes significantly. In addition, it is feasible to perform simple feature extraction operation at gateway node facilitating data security or early disease detection [25]. For example, inter-pulse interval (IPI) can be extracted [26] to facilitate arrhythmia detection as well as to generate binary sequences for entity authentication and key management in WBAN [27–30]. But these operations need to be done at the gateway node without causing a great increase in computational complexity and power consumption. Hence, there is a need to reduce the complexity of recovery operation at the gateway node. The idea of directly working on the compressed samples to find unknown parameters was introduced in Ref. [31]. [32] presents an inference framework by which the reconstruction can be avoided entirely and feature extraction techniques can be applied directly to the compressed EEG signal.

The acceptance of smartphones as mobile IoT gateways has become prominent among the research community mainly due to their (i) widespread usage, (ii) small size and relatively high computing power and (iii) seamless wireless connectivity options [33–35]. As more and more applications are running on battery driven smartphones, energy consumption becomes a critical issue. Hence, it is essential to study the energy consumption profile of smartphone, while we incorporate new IoT applications to it. Latest smartphones run on multiprocessor platforms such as ARM big.LITTLE processor that provides a wide range of energy and performance control. In Refs. [33,34], the authors discussed the performance/energy tradeoffs when running CS recovery algorithms on ARM big.LITTLE platform. In Ref. [35], the implementation of different processing frameworks on Odroid XU4 [36] evaluation board were analyzed. It has been shown that CS-based recovery can be efficiently performed on the gateway node in real time. Also the battery life of gateway node can be extended by performing basic signal processing at the gateway itself, thereby reducing transmission cost. But there is no study reported so far which evaluate the power saving at sensor nodes due to the self-configurability feature and the corresponding energy consumption at gateway node facilitating the plug and play paradigm in IoT scenario.

In this work, we present the design of a WBAN gateway node that can self-configure the sensor nodes to match the dynamics of ECG signal, while at the same time meeting the resource constraints for the telemonitoring of ECG signal. ECG monitoring applications such as healthcare (HC) and wellness (WN) applications [37] demand different signal reconstruction quality for different levels of analysis. Therefore it is highly desirable to provide different compression and quantization parameter values suiting the analysis level in energy efficient WBAN systems. Therefore, this work aims to:

1. Avoid redundant data transfer between sensor nodes and gateway nodes by addressing the diversity of system requirement in ECG telemonitoring through the design of three modes of configuration.
2. Develop a CS based self-configurable gateway node (CS-SCGN) for the telemonitoring of ECG. Fine adaptive tuning of compression and quantization parameters of the sensor node can be achieved by running the algorithm at the gateway node.
3. Through simulation studies, quantify the merits of the proposed system in terms of reduction in number of bits transmitted from the sensor node to gateway node.
4. Implement the proposed algorithm on ARMs big.LITTLE heterogeneous multiprocessor platform and evaluate the improvement in energy efficiency both at the sensor nodes and gateway node through experimental analysis.

2. Methods

2.1. Background

In this section, the concept of compressed sensing and the metrics need to be considered for performance evaluation of a CS based system, are presented.

2.1.1. Compressed sensing

CS maps the signal from a higher dimension to a lower dimension. Let $f \in \mathbb{R}^N$ be an N-dimensional ECG signal with discrete cosine transform (DCT) matrix Ψ as its sparsifying matrix and with x as its sparse representation in Ψ. i.e. $f = \Psi x$. CS encoding process involves the projection of input signal onto a $M \times N$ ($M<<N$) measurement matrix A [19].

$$y = Af = A\Psi x \tag{1}$$

In most of the prevailing CS applications [38], random matrices like Gaussian matrices, Bernoulli matrices or binary sparse matrices are used as the measurement matrices. CS recovery process involves linear programming techniques and the recovery problem can be formulated as: provided with y and A, determine the signal f in such a way that $y = Af$ is satisfied.

The limitations of dense random measurement matrices include (i) complex computation due to non-zero matrix entries, (ii) need for on-chip random seed for their generation, and (iii) slow encoding process. To overcome these limitations, sparse random measurement matrices have been suggested in Refs. [39,40]. Deterministic binary block diagonal (DBBD) matrix has been suggested in Ref. [41] for the low complex encoding of ECG signals.

Table 1
Comparison of different measurement matrices.

Matrix	Multiplication	Addition	Storage space
Gaussian	$M \times N$	$M \times (N-1)$	$M \times N$
Bernoulli	0	$M \times (N-1)$	$M \times N$
Binary sparse	0	dMN	$M \times N$
Structurally random matrix	N	$NlogN$	$2N + NlogN$
BPBD	0	$M \times (m-1) = N - M$	$M \times N$
DBBD	0	$M \times (m-1) = N - M$	0

$$A = \begin{bmatrix} \overbrace{1\ldots1}^{m} & & & \\ & \overbrace{1\ldots1}^{m} & & \\ & & \ldots & \\ & & & \overbrace{1\ldots1}^{m} \end{bmatrix} \quad (2)$$

Eqn. (2) denotes a DBBD matrix A. If A is a $M \times N$ matrix, then the compression parameter . The comparison of various measurement matrices in terms of number of additions and multiplications, and storage space is shown in Table 1 where, $M \times N$ denotes the size of the matrix and d is the number of 1's in each column of binary sparse matrix.

2.1.2. Performance metrics

The performance measures used for evaluating the signal quality are: Compression ratio (CR), Percentage root mean square difference (PRD), IPI, and Entropy.

CR is the ratio of number of samples of input signal N to the number of measurements M.

$$CR = \frac{N}{M} \quad (3)$$

PRD quantifies the distortion between the original signal f and the reconstructed signal f'.

$$\mathrm{PRD}(\%) = \frac{||f - f'||}{||f||} \times 100 \quad (4)$$

Zigel et al. [42] examined the relationship between PRD and the signal quality observed by a cardiologist. Below 2% is classified as "very good" whereas above 9% is classified as "not good/bad." The acceptable limit of PRD is less than 9%.

IPI, defined as the time difference between consecutive R peaks of an ECG signal, is an important feature of ECG signal. The randomness of bitstream generated from IPI is quantified through entropy. **Entropy** is a measure of average uncertainty in the random variable. For an n-bit binary sequence $B = \{b_1, b_2, \ldots, b_n\}$, entropy $H(B)$ is calculated as:

$$H(B) = -[p(0)\log_2 p(0) + p(1)\log_2 p(1)] \quad (5)$$

where, $p(0)$ and $p(1)$ denote the probability of occurrence of 0s and 1s respectively in B.

2.2. WBAN design

The proposed design of WBAN considers the scenario of long term ECG monitoring for health care IoT. The design is developed to provide maximum energy efficiency by incorporating three modes of operation. In a normal case, it will be only required to monitor the heart rate through IPI extraction. If a variation in heart rate is detected, there will be a need for detailed analysis of ECG signal facilitating disease detection. These two modes of operation are named as 'Monitoring mode' and 'Diagnostic mode' respectively. Providing these two modes of operation will help to prevent unnecessary high rate data transfer when it is not essential. In order to facilitate secure data transfer to protect the privacy of sensitive personal data when needed, an additional mode of operation namely 'Key generation mode' is also incorporated in the system. In each mode of operation, compression and quantization parameters are adaptively tuned to suit the signal dynamics and reconstruction quality requirements, thus optimizing the energy efficiency of the system.

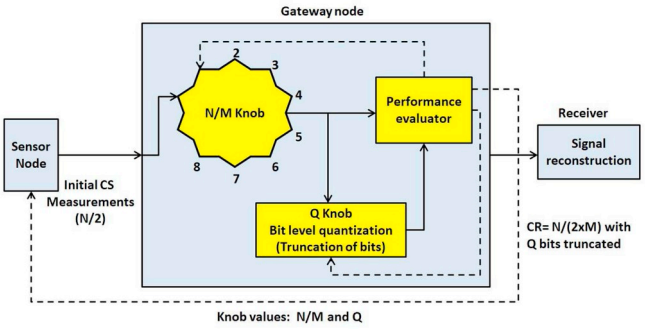

Fig. 1. Block diagram of the proposed system.

2.2.1. System model

The proposed system (Fig. 1) consists of three entities: (i) Sensor node, a biosignal sensing node that collects the biosignal (e.g., ECG), and performs compression and quantization processes on the signal. (ii) Gateway node, an intermediate node that forwards the sensor information to a remote user or a doctor and also provides real-time feedback to the WBAN user. (iii) Receiver, the entity that reconstructs the original signal for a remote user or a doctor. The sensor node can be either an on-body node or in-body (implanted) node. It captures the critical biosignals and performs the basic necessary signal processing operations with minimum hardware and computational complexity. Then the sensor node sends the quantized compressed measurements to the gateway node. The compressed measurements are quantized by just truncating the LSBs of digital values corresponding to the CS measurements. Thus the quantization module consists of an analog to digital converter followed by an LSB truncation unit. The gateway node can be either on-body (smartwatch or smartphone) or off-body (laptop or desktop computer), and it has lesser energy constraints compared to the sensor node. The gateway node collects the data coming from various sensor nodes and performs first level processing on them to provide information to the WBAN user. The gateway node then sends the data to a remote server for further processing and analysis of physiological signals.

As shown in Fig. 1, the proposed gateway node consists of three functional units: N/M knob, Q knob and performance evaluator. N/M and Q knobs tune the compression and quantization parameters of each sensor node, while the performance evaluator (Fig. 2) coordinates the entire procedure and takes the decision based on the required performance.

2.2.2. Design considerations

The two important design considerations for the CS framework in our proposed system are self-configurability and computationally

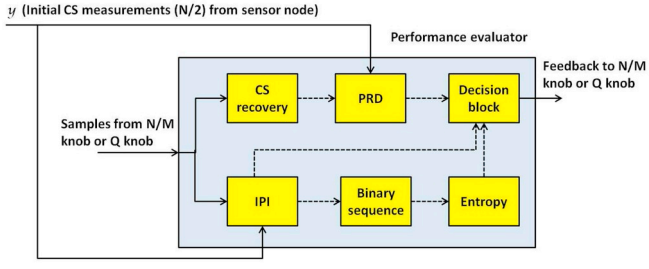

Fig. 2. Performance evaluator.

efficient design. CS framework at the sensor node should be designed in such a way that the self-configurability is achieved easily at the gateway node. The resource-constrained nature of WBAN sensor nodes demand computationally efficient design for the self-configurability feature to minimize the energy usage at the sensor node as well as at the gateway node. The factors that determine the efficiency of CS framework in our proposed system are the choice of measurement matrix and the sample length N.

2.2.2.1. Choice of measurement matrix. As WBAN sensor nodes are highly resource constrained, the most important consideration is to make the CS encoding process as simple as possible. Therefore, we have to choose a measurement matrix in CS based encoding for ECG telemonitoring such that:

a) The encoder design is low complex and energy efficient.
b) The overall WBAN system is reconfigurable in response to application requirements or biosignal dynamics with minimum computational complexity.
c) The reconstruction algorithm is simple and its running time is less.

Since DBBD matrix in CS framework offers low computational complexity and memory requirement compared to other measurement matrices (see Table 1), it is highly recommended for the design of resource constrained systems. In the design of energy efficient sensor nodes, where the compression ratio can be tuned by gateway node, DBBD is the best choice due to the following additional property.

Proposition 1. *Measurements corresponding to higher compression ratio can be generated through simple addition of DBBD based encoder output.*

Proof. *Consider a DBBD based CS encoder with input* $f = [f_1, f_2, ..., f_N] \in \mathbb{R}^N$ *and output* $y = [y_1, y_2, y_3, ..., y_M] \in \mathbb{R}^M$. *To have the measurements y corresponding to CR* = 2, *m must be equal to* 2 *in* Eqn. (2). *Thus,* $y = [f_1 + f_2, f_3 + f_4, ..., f_{N-1} + f_N] \in \mathbb{R}^{N/2}$. *For CR* = 4, $y' = [f_1 + f_2 + f_3 + f_4, ..., f_{N-3} + f_{N-2} + f_{N-1} + f_N] \in \mathbb{R}^{N/4}$. *No other matrices have the feature of generating higher order CS measurements from its lower order measurements, this way*. □

From Table 1, it is evident that DBBD matrix has lower complexity and higher energy efficiency (design criterion *a*). Reconfigurability can be easily realized by employing DBBD matrix in CS encoding as demonstrated in Prop. 1 (design criterion *b*). The CS recovery algorithm presented in Ref. [41] is simple and fast, which exploits the properties of DBBD matrix through thresholding in the DCT domain (design criterion *c*). Hence, we choose DBBD matrix as the measurement matrix in our proposed system.

2.2.2.2. Choice of N value. Usually, the data length N is taken as power of 2 such as 256, 512, etc. to match the block length requirements for various signal processing operations including FFT. In Ref. [43], the author pointed out that there are good FFT algorithms with any block length. Most of the common algorithms in Ref. [44] support a wider class of block lengths, and those algorithms have lesser computational complexity compared to those having power of two as block lengths. If we take $N = 512$ in a DBBD based CS encoding, then m can take only values 2, 4, 8, 16, etc. This discontinuity in the range of values that the compression parameter can take, is a drawback for the practical design of a system with self-configurability feature. Choosing N as a highly composite number (HCN) solves this issue.

Proposition 2. *If the signal length N for a DBBD based CS scheme is a highly composite number (i.e., 840), then the compression parameter m can take maximum number of integer values as operating points.*

Proof. *HCN is a positive integer that has more divisors than any other smaller integer* [45]. *HCNs are listed in the sequence* A002182 *of OEIS* (*online encyclopedia of integer sequence*). *In engineering designs, these numbers tend to simplify the calculations involving fractions.*

840 is a highly composite number and is the least common multiple of 2, 3, 4, 5, 6, 7 and 8. Therefore, in an $M \times N$ *DBBD matrix, if we take* $N = 840$, *we can avail different m values such as 2, 3, 4, 5, 6, 7, 8, 10, 12, 14, 15, 20, 21, 24, 28, 30 etc. Also except 1260, all the other succeeding HCNs after 840 are multiples of 840. Therefore* $N = 840$ *is a good choice for DBBD based CS scheme.* □

Using the signal length N as HCN, the proposed tuning method for compression parameter has many advantages such as lack of need for buffer and better power efficiency compared to the padded BPBD method explained in Ref. [23].

2.2.3. Functional blocks in CS-SCGN

2.2.3.1. N/M knob. The N/M knob is adjusted to generate CS measurements corresponding to different compression ratios from the initial measurements reaching the gateway node. Let the initial measurements reaching the gateway node with CR = 2 from the sensor node be m_1, m_2, m_3, …, m_{420}. Now in order to generate the measurements corresponding to CR = 4 at the gateway node, it is sufficient to add two consecutive measurements (i.e., $m_1 + m_2$, …, $m_{419} + m_{420}$). To procure measurements with CR = 6, three consecutive initial measurements (i.e., $m_1 + m_2 + m_3$, …, $m_{418} + m_{419} + m_{420}$) are added and so on. If the measurements m_1, m_2, m_3, …, m_{280} arriving the gateway corresponds to CR = 3, then the two consecutive measurements are added (i.e., $m_1 + m_2$, …, $m_{279} + m_{280}$) to get the measurements corresponding to CR = 6. For the measurements with CR = 9, the three consecutive measurements are added (i.e., $m_1 + m_2 + m_3$, …, $m_{278} + m_{279} + m_{280}$) and so on. After adjusting the N/M knob in steps, the resulting measurements are fed to the performance evaluator for signal quality assessment.

2.2.3.2. Quantization knob. The input fed to the Q knob is the CS measurements corresponding to the optimum CR value fixed by the action of N/M knob. Then the Q knob will perform bit-level truncation by removing LSBs one by one from the input CS measurements. After each truncation, the Q knob outputs the resulting measurements to the performance evaluator which will decide whether to continue truncation or not, based on a quality metric. Thus N/M and Q knobs are operated in succession at the gateway node so as to find the optimum compression and quantization parameters achievable at the sensor node.

2.2.3.3. Performance evaluator. The PRD, IPI, and entropy blocks in the performance evaluator (Fig. 2) measures the corresponding quality metric and the decision block will provide feedback to N/M and Q knobs for adjusting the compression and quantization parameters respectively. The binary sequence block generates a bit sequence from the extracted IPIs. The final parameter values are then conveyed to the sensor node. The performance evaluator compares the received initial CS measurements from the sensor node with the measurements corresponding to the successive knob outputs.

2.2.4. Modes of configuration

The three modes of configuration (Fig. 3) which facilitate plug and play operation of the proposed system are (i) diagnostic mode, (ii) monitoring mode, and (iii) key generation mode. Each mode consists of three events E1, E2, and E3 as shown in Fig. 3a. In event E1, the sensor node performs basic initial compression with CR = 2, and then forwards the compressed measurements to the gateway node. In event E2, the self-configurable gateway node will find the optimum knob values and send those values to the concerned sensor node for updating. The parameters are updated at the sensor node based on the feedback from gateway in event E3, and then the required mode of operation is activated. Events E1 and E3 remain the same for all the modes. Depending on the mode selected, E2 will vary to accommodate the associated

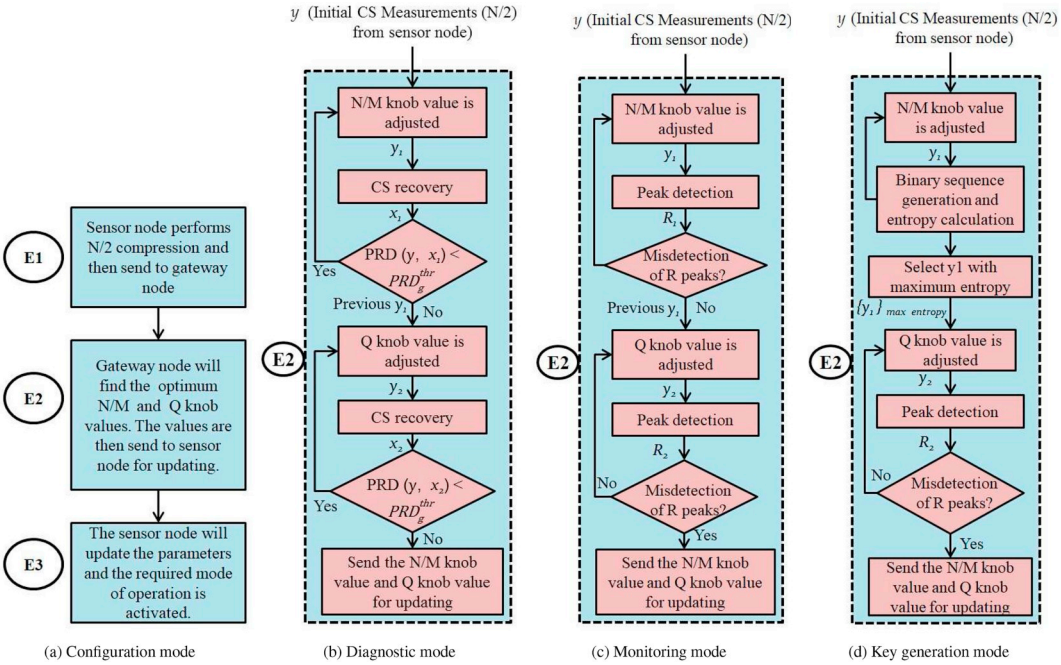

Fig. 3. Modes of configuration.

performance metric. It can be clearly seen from Fig. 3 that the diagnostic mode operation is based on PRD value, monitoring mode is based on IPI value, and the key generation mode is based on entropy value. After the configuration settings are updated and saved, the settings can be checked and updated on a periodic basis or on demand by the remote healthcare provider.

2.2.4.1. Diagnostic mode. This mode provides a detailed interpretation and measurement of ECG signal. Various CVDs such as sinus arrhythmia, sinus tachycardia, myocardial infarction, etc. require a high level of signal quality for diagnosis and treatment. The performance metric employed in this mode is PRD level. CS recovery is performed by using a simple and fast recovery method presented in Ref. [41]. Upon receiving the compressed measurements with CR = C (initially, $C = 2$) from the on-body node, the gateway node performs the compression using N/M knob on the received measurements to find the largest CR value (CR_1) that keeps the corresponding PRD_g below the acceptable limit PRD_g^{thr} as shown in Fig. 3b. Then the gateway node will inform the final possible CR value (CR_1) to the on-body node, and the on-body node will perform compression with net CR, $CR' = C \times CR_1$. If the PRD_g corresponding to CR_1 is lesser than the threshold PRD_g^{lower} at the gateway node, then the final CR' will be one added to the previous CR'. The Q knob is provided with CS measurements obtained after adjusting N/M knob to have CR = CR_1. Then the knob will truncate LSBs bit by bit and compute the respective PRD_g values. When the PRD_g value exceeds the acceptable limit, then the gateway node will stop truncating and informs the Q knob value to the sensor node.

2.2.4.2. Monitoring mode. This mode is mainly intended for heart rate monitoring. This mode will be enough to monitor the health status of a healthy person during activities such as sports or exercise. This mode works based on features extracted from ECG that can inform about the general health status of the user. Among the ECG features, the most prominent one is RR interval (also referred as IPI) which is commonly employed for disease diagnosis as well as for cryptographic key generation. PRD values can go beyond 9% without affecting the basic morphology of signal. Hence, in this mode, the IPI values are used for evaluating the performance as shown in Fig. 3c. In monitoring mode, the IPI block in the performance evaluator extracts the IPI values from the initial CS measurements as well as from the knob adjusted measurements using Pan Tompkins method [46] for ECG QRS detection. Here, the gateway node varies the knob values and checks whether a peak is missed or a fake peak is detected in relation to that of the initially received CS measurements from the sensor node. The decision block decides whether to continue adjusting the knob values in gateway node or to inform the sensor node about the optimum possible knob values. If the extracted IPI values indicate any type of disorder in health condition, the mode will be switched to diagnostic mode.

2.2.4.3. Key generation mode. This mode is meant for the generation of a secret random key using IPI values for securing the transmission of physiological signal. For cryptographic key generation from IPIs, there is no need to check whether the required PRD level is met or not. In key generation mode, 128-bit binary sequence is generated by concatenating selected bits (four LSBs) from each 32 IPI values [28,30]. Instead of PRD values, the performance evaluation is based on the entropy of the sequence for different knob values as shown in Fig. 3d. The knob values corresponding to maximum entropy are selected and conveyed to the sensor node by the decision block in the performance evaluator.

2.2.5. Application to the telemonitoring of multi-lead ECG (MECG) signals

The performance of the proposed system can be well evaluated by adopting it in the telemonitoring of MECG signals. The standard MECG signal consists of 12 leads - I, II, III, aVR, aVL, aVF, V1, V2, V3, V4, V5, and V6. Eight leads (I, II, V1, V2, V3, V4, V5, and V6) are independent whereas other leads are derived ones. The sensor node corresponding to each lead performs compression via CS using DBBD matrix and quantization via bit level truncation. The gateway node then finds the required parameters for each lead of MECG. The whole system can be depicted as in Fig. 4. The gateway node informs the required parameters to each sensor node depending on the configuration mode selected.

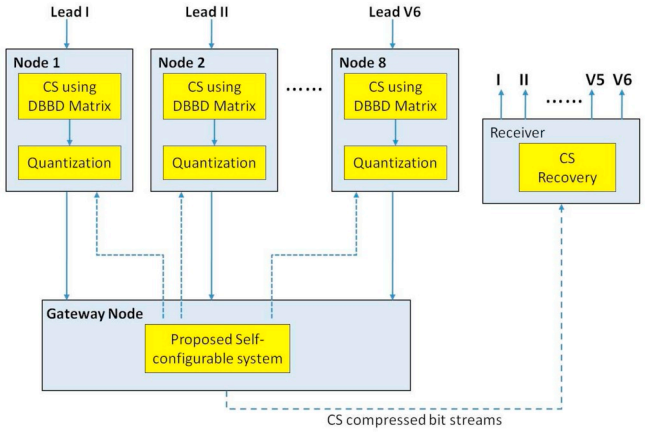

Fig. 4. Proposed self-configurable system in telemonitoring of MECG.

3. Results

3.1. Experimental setup and parameter settings

ECG data is taken from the MIT PhysioBank database (http://www.physionet.org/physiobank). Experiments were carried out on the ECG data from 150 subjects: 48 subjects (360 Hz) from MIT-BIH Arrhythmia database (MITDB) [47], 79 subjects (250 Hz) from European ST-T database (EDB) [48], and 23 subjects (250 Hz) from MIT-BIH Atrial Fibrillation database (AFDB) [47]. MECG data is taken from PTB Diagnostic ECG database [47] that contains 549 records from 290 subjects, sampled at 1 KHz with 16-bit resolution. Each record in MITDB database consists of two leads with slightly over 30 min long. Modified limb lead II (MLII) in MITDB record is used in our simulation studies. For MITDB database, a base offset value of 1024 is subtracted from each sample values. For simplicity, the 48 records in MITDB database are numbered from 1 to 48 in the order in which they are present in the database. The individual recordings of EDB database are for 2 h in duration. Lead V4 signal is used in our simulation. Each record in AFDB database is 10 h in duration and one of the ECG signal ECG1 is employed for simulation. Out of the 16 leads in the PTB database record '*s0001_rem*', 8 independent leads are used as MECG data in the simulation process. No pre-processing operations are performed on the database records prior to simulation study. The experiments are conducted in MATLAB R2017A, with 3.3 GHz Intel Xeon processor. Throughout the experiments, DCT is employed as the sparsifying basis.

3.1.1. Effect of DBBD based CS on the ECG compression

Fig. 5 illustrates that compression ratio achieved by DBBD matrix within the acceptable limit (PRD = 9%) is far better than that by binary sparse matrix. Fig. 6 shows the effect of DBBD matrix in various ECG datasets. The average PRD is calculated over the entire records of a particular database. Even at high CRs, the ECG signal can be reconstructed without significant losses. One of the disadvantages of

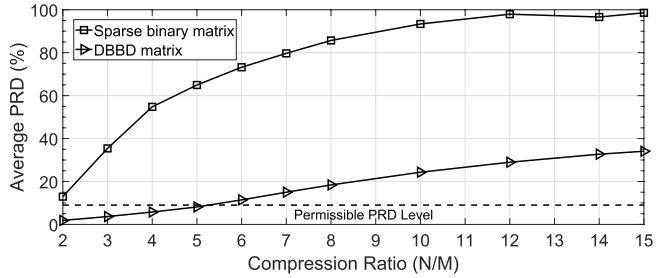

Fig. 5. PRD averaged over the entire MITDB database for various compression ratios using DBBD matrix and sparse binary matrix.

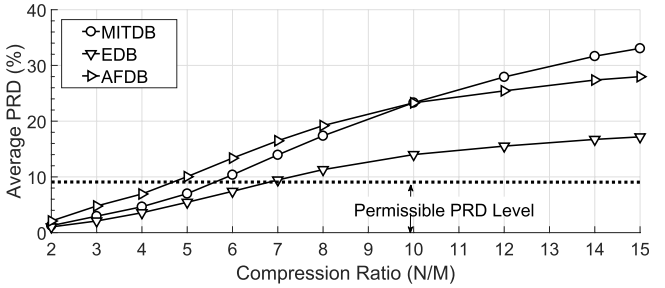

Fig. 6. PRD averaged over all the records in three different datasets for various compression ratios using DBBD matrix.

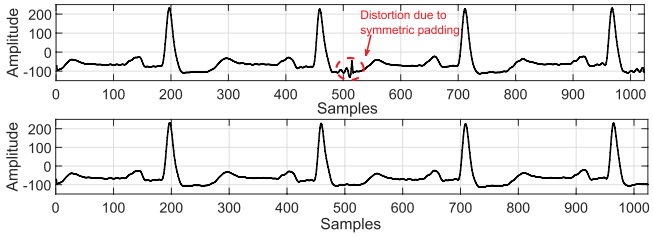

Fig. 7. First 1024 samples of ECG signal record 105 from MITDB database that are reconstructed following the padding method in Ref. [23] with $N = 512$ (Top) and the proposed tuning method with $N = 840$ (Bottom). For both the cases, CR is taken as 5. The distortion due to symmetric padding is shown in circle.

tuning method for compression parameter [23] using padded BPBD matrix is illustrated in Fig. 7. At the padding region, the reconstructed signal has distortions that may result in serious faults. The effect of bit level quantization by truncating (removing the LSBs) the CS measurements is shown in Fig. 8. Mean PRD is calculated for 48 subjects from MITDB database. Fig. 8 demonstrates the variation of mean PRD with different number of LSBs removed for CR = 2 and CR = 5. It is clear from the figure that the removal of 4–5 LSBs will not degrade the signal below the diagnostic standard, for a CR up to 5.

3.1.2. Extraction of IPIs

IPIs can be extracted from the CS measurements by applying Pan Tompkins method for ECG QRS detection. The QRS detection algorithm is applied directly on compressed samples without any intermediate processing as shown in Fig. 9. The QRS peaks detected directly from the measurements as shown in Fig. 9b exactly match with those detected from the original signal (Fig. 9a). In many cases, it is sufficient to transmit only one bit (MSB) of compressed measurements for the effective R peak detection. Fig. 10a and Fig. 10b correspond to the original signal and one-bit quantized measurements respectively for MITDB record '119'. The abnormality of signal at the 4^{th} peak can be identified directly from the measurements. There is a drastic change in the 3^{rd} IPI compared to the 1^{st} and 2^{nd} IPIs. Thus, the system can identify the abnormality of signal directly from the one-bit CS measurements.

3.2. Simulation of proposed algorithm

A major part in simulation analysis of proposed reconfigurable system is to arrive at the threshold values of PRD at the gateway node, which can give a satisfactory performance. Since the original signal is not reconstructed at the gateway node and the performance is evaluated between the initially compressed signal y from the sensor node with CR = 2 and the signal reconstructed from those with higher order CRs obtained from y, the permissible PRD level at the gateway node PRD_g^{thr} is different from that at the sensor node (9%). Another part in simulation study is to quantify the reduction in number of transmitted bits from the sensor node to the gateway node as a result of self-

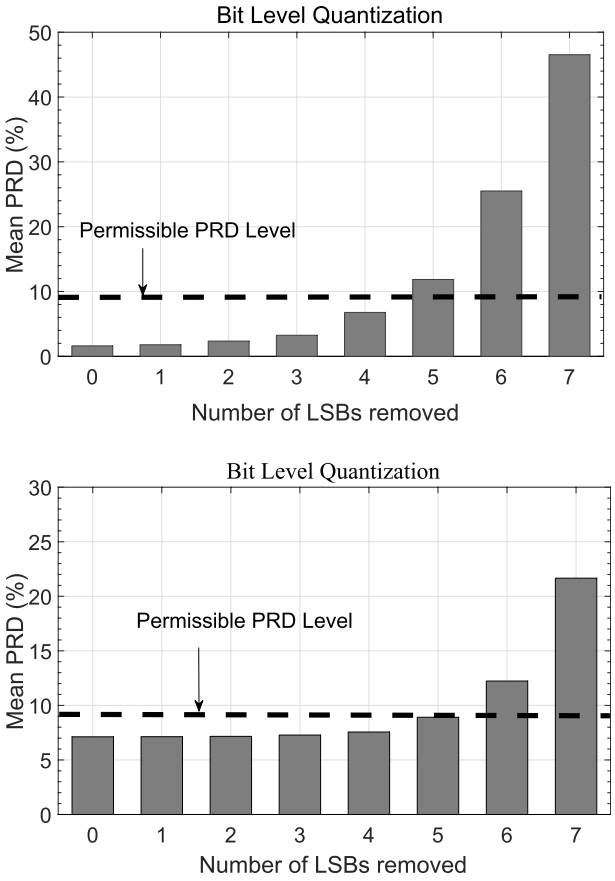

Fig. 8. PRD averaged over all MITDB ECG records for different bit level truncations (number of LSBs removed). The limit of permissible PRD level is shown in dotted lines. CR = 2 (top) and CR = 5 (bottom).

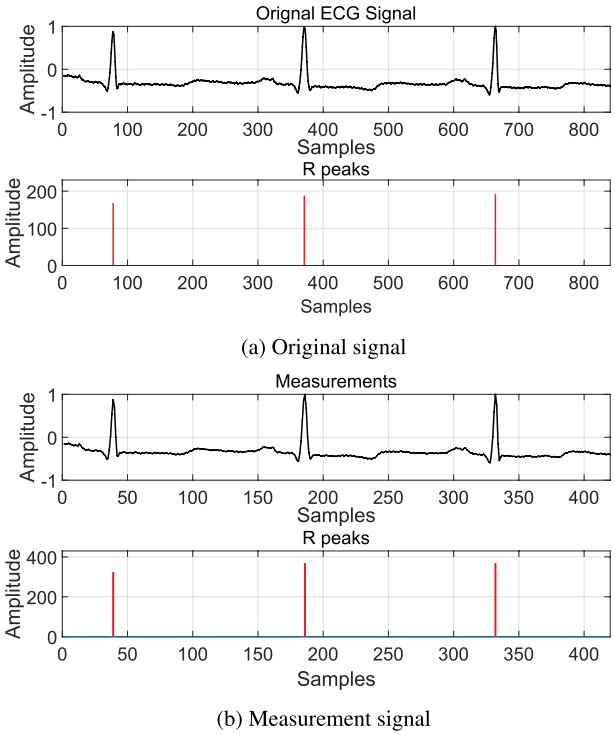

(a) Original signal

(b) Measurement signal

Fig. 9. Detection of R peaks from original signal and measurement signal with $N = 840$ and $M = 420$ using Pan Tompkins QRS detection algorithm.

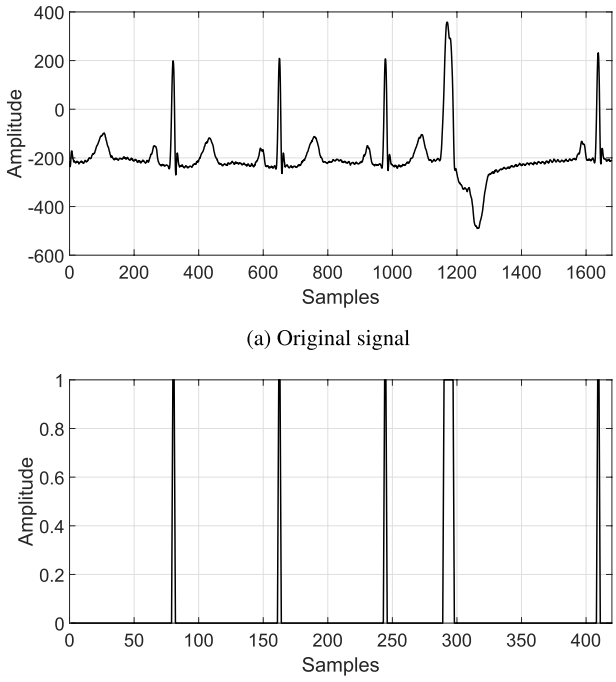

(a) Original signal

(b) Measurement signal

Fig. 10. R peak detection from the compressed signal $M = N/4$ with 1 bit quantization for the MITDB record 119. The abnormality in the signal after the third peak is clearly visible from the measurement signal.

configurability in different modes. Finally, we also quantify the bit savings when the proposed configurable gateway system is applied for the telemonitoring of MECG signals.

The working of N/M knob is demonstrated using Table 2 and Table 3 with 12 subjects from MITDB database. The PRDs in bold correspond to PRD associated with the maximum possible compression ratio having an acceptable signal quality for each record in diagnostic mode. For the record '106′, the on-node compression of CR = 2 results in a PRD of 1.84%. At the gateway node, the compression of CR = 2 results in PRD_g = 8.32% as shown in Table 2. If the gateway node takes 9% as PRD_g^{thr}, then it will convey the sensor to go for CR = 2 × 2. However, at the sensor node, CR = 4 results in a PRD = 9.29% (Table 3) which is beyond the diagnostic threshold level (9%). By checking the records '106′, '108′, '118′, and '221′, we conclude that the threshold PRD_g at the gateway node cannot be 9%. Through experimentation, it was found that the proposed algorithm works properly with the PRD_g^{thr} as 8%. Also, we noted that if the PRD_g corresponding to the maximum possible CR at the gateway node is less than a lower threshold PRD_g^{lower}, then one is added to the final CR value at the sensor node. On verifying some of the records '101', '103', and '119', we found that PRD_g^{lower} = 5% gives good results.

The working of Q knob is illustrated by showing the quantization effect at the gateway node (Table 4) and at the on-body sensor node (Table 5). For the record '108', PRD_g corresponding to the truncation of 5 bits at the gateway node is 5.23%. The Q knob value $i = 5$ is conveyed to the sensor node. Then the sensor node will perform truncation of 5 bits before transmitting to the gateway node resulting in a PRD of 5.67%, which is well within the permissible PRD level. The record '114' shows the significance of setting 8% as the PRD_g threshold at the gateway node. PRD_g of 8.3% at the gateway node corresponds to 9.09% at the sensor node which exceeds the permissible PRD level. But PRD_g less than 8% at the gateway node is well within the permissible PRD level (< 9%) at the sensor node.

In the case of monitoring mode, IPIs extracted from the initial CS measurements received at the gateway node from sensor node (IPIs

Table 2
PRD_g values for MITDB ECG records at the gateway node with the variation in N/M knob values corresponding to the respective CS measurements (CR = 2) from the sensor node.

ECG	On body node	Gateway node							
	CR = 2	CR = 2	CR = 3	CR = 4	CR = 5	CR = 6	CR = 7	CR = 8	CR = 10
100	1.25	**5.08**	13.77	23	29.52	33.92	35.48	38.29	39.18
101	1.34	**4.07**	12.04	20.46	26.56	29.4	33.16	34.75	37.75
103	1.09	**3.6**	13.69	30.09	39.97	47.13	52.14	54.84	59.6
105	1.16	2.65	3.59	**7.74**	13.44	19.16	24.43	32.27	37.18
106	1.84	**8.32**	13.76	30.44	41.8	48.81	51.94	54.43	61.13
107	0.56	3.28	**6.24**	9.47	11.85	13.07	16.05	16.49	20.72
108	1.4	3.97	4.67	5.71	6.66	7.89	**8.67**	12.89	15.33
114	2.11	**6.2**	14.08	20.38	21.44	21.16	20.82	20.91	21.98
118	0.49	1.84	5.7	8.02	**8.75**	9.91	13.05	15.23	21.44
119	0.54	1.31	**4.27**	9.54	13.79	15.66	17.69	19.58	20.9
122	0.61	1.5	4.16	5.07	**8.56**	13.28	16.04	19.02	24.28
221	1.45	3.59	**8**	15.96	22.97	29.67	36.11	41.23	44.85

Table 3
PRD corresponding to different CRs at the sensor node.

ECG	On body node									
	CR = 2	CR = 3	CR = 4	CR = 5	CR = 6	CR = 7	CR = 8	CR = 10	CR = 12	CR = 14
100	1.25	2.6	**5.62**	9.5	14.41	19.01	23.64	30.11	34.48	36.02
101	1.34	3.06	4.58	**7.68**	12.63	17.78	21.05	27.12	29.93	33.66
103	1.09	3.08	4.08	**7.82**	14.25	22.32	30.72	40.57	47.69	52.65
105	1.16	2.86	3.09	3.11	3.98	5.39	**8.04**	13.72	19.42	24.68
106	1.84	**4.95**	9.29	9.7	14.61	24.4	31.22	42.5	49.44	52.54
107	0.56	1.97	3.63	5.07	6.59	**7.39**	9.8	12.16	13.36	16.32
108	1.4	3.98	4.56	4.89	5.23	6.06	6.21	7.11	8.29	**9.05**
114	2.11	6.03	**7.1**	10.54	14.93	18.86	21.17	22.19	21.92	21.59
118	0.49	0.94	2.06	4.31	5.99	7.56	8.31	**9.02**	10.17	13.28
119	0.54	0.73	1.5	2.62	4.49	**6.81**	9.79	14.04	15.9	17.93
122	0.61	1.19	1.74	2.53	4.38	5.32	5.28	**8.76**	13.47	16.22
221	1.45	3.63	4.19	5.9	**8.56**	12.32	16.44	23.41	30.09	36.5

Table 4
PRD_g values for MITDB ECG records at the gateway node with the variation in quantization knob values corresponding to the respective CS measurements (CR = 2) from the sensor node.

ECG	Gateway node								
	i = 0	i = 1	i = 2	i = 3	i = 4	i = 5	i = 6	i = 7	i = 8
100	4.86	4.87	5.03	4.97	**5.45**	11.94	19.29	14.75	83.27
101	4.92	4.94	4.93	5.63	**5.36**	12.37	9.74	45.05	25.52
103	3.25	3.25	3.30	4.10	5.16	7.75	**6.85**	34.87	62.60
105	2.61	2.63	2.68	3.56	3.13	**5.40**	10.73	36.76	61.96
106	8.47	8.47	8.49	**8.61**	9.89	9.57	13.42	23.91	82.29
107	3.26	3.26	3.27	3.32	4.02	4.92	**4.61**	9.72	22.37
108	3.48	3.49	3.70	3.60	6.18	**5.23**	20.15	34.33	63.25
114	6.95	6.96	6.98	**7.23**	8.30	11.89	21.25	34.38	54.01
118	2.35	2.35	2.39	2.38	2.84	2.69	7.08	**5.83**	27.57
119	1.01	1.01	1.08	1.20	1.18	3.34	5.59	**4.81**	12.12
122	1.70	1.71	1.74	1.84	1.83	2.60	9.29	**7.56**	34.88
221	3.69	3.72	3.75	3.96	4.93	**7.49**	12.64	43.24	30.96

Table 5
PRD corresponding to bit level quantization at the sensor node.

ECG	On body node								
	i = 0	i = 1	i = 2	i = 3	i = 4	i = 5	i = 6	i = 7	i = 8
100	5.37	5.38	5.52	5.48	**5.92**	12.16	19.42	14.98	83.15
101	5.52	5.54	5.52	6.16	**5.92**	12.61	10.16	45.06	25.68
103	3.74	3.74	3.79	4.49	5.49	7.98	**7.17**	34.89	62.52
105	3.02	3.03	3.07	3.87	3.49	**5.65**	10.91	36.80	62.02
106	9.58	9.58	9.60	9.70	10.85	10.60	14.21	24.40	82.11
107	3.60	3.60	3.61	3.66	4.30	5.17	**4.91**	9.96	22.62
108	4.02	4.03	4.22	4.12	6.51	**5.67**	20.31	34.51	63.54
114	7.87	7.88	7.89	**8.11**	9.09	12.50	21.68	34.65	54.23
118	2.61	2.61	2.65	2.64	3.06	2.94	7.20	**6.05**	27.66
119	1.18	1.18	1.25	1.35	1.34	3.40	5.65	**4.95**	12.24
122	1.96	1.97	2.00	2.09	2.08	2.80	9.37	**7.77**	34.96
221	4.31	4.34	4.36	4.55	5.44	**7.88**	12.90	43.27	31.15

corresponding to CR = 2 in Table 6) is compared with the CS measurements at gateway node for different N/M knob values as shown in Table 7. For the MITDB record '100', since the peaks are misdetected for CR = 14 at the gateway node, it will convey the sensor node to go for CR = 2 × 12 = 24. Thus the required N/M value at the sensor node, i.e., $(N/M)_S$ is 24. Similarly, the bit resolution required at the sensor node $(Q)_S$ is found to be 7. For key generation mode, the entropy of binary sequences generated from the IPI values is computed for different values of N/M at the gateway node. Table 8 illustrates that the entropy of binary sequences extracted from different segments (S1, S2, …, S10) of an ECG record remains almost the same for a particular CR. Initially, the gateway node will find the entropy of sequences up to CR = 10 and then the higher N/M knob value for which the entropy is closer to 1 (> 0.99), is conveyed to the sensor node. For the record '100', $(N/M)_S$ and $(Q)_S$ values in the key generation mode are found to be 6 and 8 respectively.

Fig. 11 shows the number of bits transmitted with a sample length 840 in different modes for the entire records of MITDB database. The MITDB record number indicates the number/position at which a particular record is present in the database. i.e., record number 1 indicates the record '100', 2 indicates record '101', and so on. The 'non-self-configurable' mode indicates the parameters that are chosen common to all modes, all leads, and all individuals to give acceptable quality metric. For the non-configurable mode, $(N/M)_S$ and $(Q)_S$ are taken as 2

Table 6
Extraction of IPIs from the original ECG signal with different CRs at the sensor node for the MITDB record '100'.

CR	IPI values of record 100									
	IPI1	IPI2	IPI3	IPI4	IPI5	IPI6	IPI7	IPI8	IPI9	IPI10
2	147	146	142	142	142	147	118	179	152	146
4	73	73	71	71	71	74	59	89	76	73
6	49	49	47	48	47	49	39	60	51	48
8	37	36	36	35	36	37	29	45	38	36
10	30	29	28	29	28	29	24	36	30	29
12	24	25	23	24	24	24	20	30	25	24
14	21	21	20	20	21	21	17	25	22	21
20	15	15	14	14	14	15	12	18	15	14
24	12	12	12	12	12	12	10	15	12	12
28	10	10	*	21	10	9	12	11	11	*

Table 7
Extraction of IPIs from the compressed measurement signal with different CRs at the gateway node for the MITDB record '100'.

CR	IPI values of record 100									
	IPI1	IPI2	IPI3	IPI4	IPI5	IPI6	IPI7	IPI8	IPI9	IPI10
2	73	74	71	71	71	73	59	89	76	73
4	37	37	35	36	35	37	29	45	38	36
6	24	25	24	23	24	24	20	30	25	24
8	19	18	18	17	18	19	14	23	19	18
10	15	15	14	14	14	15	12	18	15	14
12	12	12	12	12	12	12	10	15	12	12
14	10	10	*	21	10	9	12	11	11	*

and 12 respectively. From Fig. 11, it is evident that there is a considerable reduction in the number of bits required to be transmitted from the sensor node in various modes in the proposed system, which makes the system highly energy-efficient.

The application of proposed self-configurable system for use in the telemonitoring of MECG signal is carried out using MECG data from PTB database. 840 samples are taken from each channel of dataset record '*s*0001_*rem*'. After running the proposed algorithm in diagnostic mode, we obtained the possible $(N/M)_S$ and $(Q)_S$ values as shown in Table 9. The $(N/M)_S$ and $(Q)_S$ values for each lead are found to be varying from 2 to 14, and 7 to 10 respectively. The percentage of bit saved is computed with reference to the non-self-configurable mode settings and we can see that there are considerable savings in the bit transmitted using the proposed self-configurable gateway node. Thus instead of assigning the parameter values manually, we can operate the continuous telemonitoring of MECG in a plug and play manner.

3.3. Hardware implementation

We implemented the IoT gateway node on Hardkernel's Odroid XU4 board, featuring Samsung Exynos 5422 Cortex A15 and A7 Octacore CPU as shown in Fig. 12. Their architecture featuring ARMs big.LITTLE heterogeneous multi-processing (HMP) platform can be found in latest smartphones (Samsung Galaxy S5). Thus the XU4 board can be effectively used as a gateway for realizing the scenarios employed for real-time health monitoring. The gateway node is externally equipped with an XBee S2C embedded RF module for acquiring data from the sensor node and a Wifi Dongle 802.11n for forwarding received data to the cloud. The algorithms are implemented in Python language operating on Ubuntu 16.04. Energy consumption is measured by placing a current probe in series with the power source of gateway and then logging the readings using digital storage oscilloscope. The gateway battery lifetime for various data processing frameworks is estimated based on a 10.78 Wh battery [34,35], present in latest smartphones. ARM Streamline Performance Analyzer is used to provide an accurate graphical representation of gateway system resources.

Firstly, the energy efficiency of the simplified CS recovery algorithm [41] compared to OMP algorithm is substantiated. Then in order to find the feasibility of proposed algorithm, we determine the energy required for performing primary processing tasks, configuration of different modes, and transmission and reception using XBee and WiFi modules. The advantage of using the proposed self-configurable system is evaluated by figuring out the extension in battery life of the sensor node

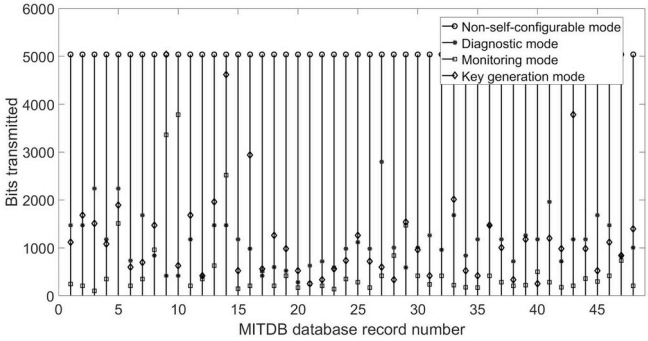

Fig. 11. Bits transmitted from sensor nodes in different modes for the 48 records in MITDB.

Table 9
Effect of proposed self-configurable algorithm on MECG signals in diagnostic mode.

Leads	I	II	V1	V2	V3	V4	V5	V6
$(N/M)_S$	4	2	14	8	7	7	7	8
PRD	8.37	7.26	8.89	7.41	8.02	8.37	8.74	8.60
$(Q)_S$	8	7	10	8	8	8	8	8
PRD after truncation	8.41	8.46	8.91	8.44	8.31	8.51	8.94	8.75
Bits saved (%)	66.67	41.67	88.1	83.3	80.95	80.95	80.95	83.33

Table 8
Entropy of binary sequences generated from extracted IPI values for the MITDB record '100' with different CRs.

CR	Entropy of binary sequences generated from IPI of record 100										
	S1	S2	S3	S4	S5	S6	S7	S8	S9	S10	Average
1	0.9422	0.935	0.9422	0.954	0.9745	0.948	0.954	0.94	0.965	0.97	0.949
2	0.9422	0.935	0.9355	0.948	0.97	0.948	0.949	0.94	0.96	0.96	0.946
3	0.8464	0.868	0.8571	0.857	0.8234	0.857	0.811	0.86	0.846	0.84	0.847
4	0.9993	0.997	0.9993	0.999	0.9998	0.999	1	1	1	1	**0.999**
5	0.9857	0.974	0.9786	0.991	0.9857	0.986	0.986	0.99	0.989	0.98	0.984
6	0.9984	0.994	0.9972	0.991	0.9972	0.991	0.997	0.98	0.997	0.99	**0.993**
7	0.97	0.97	0.9786	0.96	0.97	0.965	0.97	0.95	0.965	0.97	0.967
8	0.9786	0.979	0.9786	0.986	0.9823	0.982	0.982	0.98	0.974	0.97	0.981
10	0.9823	0.96	0.9786	0.96	0.9745	0.96	0.97	0.96	0.96	0.96	0.968

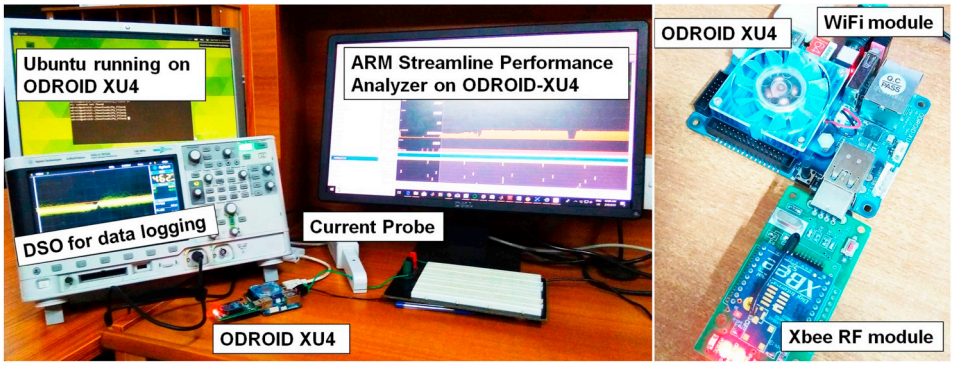

Fig. 12. Hardware implementation setup.

Table 10
Energy and recovery time per window ($N = 840$) for OMP and simplified CS recovery [41] at the gateway node.

Frequency [MHz]	OMP				Simplified CS recovery [41]			
	Energy (J)		Reconstruction time (s)		Energy (J)		Reconstruction time (s)	
	A15	A7	A15	A7	A15	A7	A15	A7
800	1.267	0.614	2.167	3.07	0.085	0.088	0.1626	0.631
1000	1.290	0.871	1.780	2.68	0.093	0.103	0.1329	0.5125
1200	2.356	1.223	1.540	2.44	0.104	0.121	0.1126	0.426
1400	2.555	1.289	1.385	2.283	0.178	0.149	0.097	0.369
1600	2.768	–	1.262	–	0.204	–	0.087	–
1800	3.261	–	1.167	–	0.225	–	0.078	–

considering the transmission cost for the entire subjects in MITDB database.

Table 10 shows the energy consumption at the gateway node for two CS recovery algorithms namely orthogonal matching pursuit (OMP) algorithm [49] and the faster CS recovery algorithm of [41] with different core frequencies. The table indicates that the simplified CS recovery attributed by the property of DBBD matrix employed in our proposed system consumes much less energy compared to OMP. Thus we can ascertain that the CS recovery operations in the diagnostic mode will not burden the system energy. Table 11 summarizes the gateway's energy and battery lifetime for running the three configuration modes on the MITDB ECG signal record '100'. The configuration of different modes requires only less energy to determine the parameters.

A free multi-platform application XCTU [50] is employed in our system to configure and manage Xbee modules. The XBee module connected to the host computer is made to communicate with that on the ODROID board. Dropbox, a cloud storage service is modeled as a remote server. The gateway node performs the communication with the Xbee module and Dropbox through Python scripts. It has been found that the gateway node consumes 0.147 mJ/bit and 9.23 μJ/bit for communicating data to and from the sensor node respectively. Also, the energy consumption for uploading data to the cloud is determined.

In Ref. [35], the compressed ECG signal from the sensor node has to be reconstructed using OMP algorithm before it could be analyzed. After analysis, the data are transmitted to the cloud once in every 3 s. In our proposed system, the features can be extracted directly from the compressed samples without CS recovery due to the morphological retaining property of DBBD matrix, and conveyed to the cloud periodically or upon user request.

To facilitate the calculation of energy consumption on sensor node, we model the sensor node transceiver as a wireless biosignal acquisition system-on-a-chip (SoC) proposed in Ref. [51], which is specifically meant for IEEE 802.15.4 (ZigBee) applications. The transmitter consumes 93 nJ/bit with a data rate of 250 kbps and a supply voltage of 1.2 V. We consider that the sensor node is powered by a 4500 mAh battery [35].

Now consider that a vendor is providing standard sensor nodes with a fixed compression ratio and bit-level quantization. Considering 48 subjects of MITDB database, the common acceptable compression ratio and the number of bits required for diagnostic mode are found to be 3 and 10 respectively. Similarly, for monitoring mode and key generation mode, they are found to be 2 and 9, and 2 and 12 respectively. The self-configurability will increase the battery lifetime of a sensor node in various modes as shown in Fig. 13, since the transmission costs from the sensor node to gateway node is reduced significantly compared to the

Table 11
Total energy for configuring different modes at the gateway node for the MITDB record '100'

Performance Parameter	Core	Frequency [MHz]	Diagnostic Mode	Monitoring Mode	Key Generation Mode
Energy (J)	A7	800	1.454	0.099	0.0848
		1400	1.674	0.120	0.119
	A15	800	2.194	0.137	0.147
		1400	3	0.254	0.232

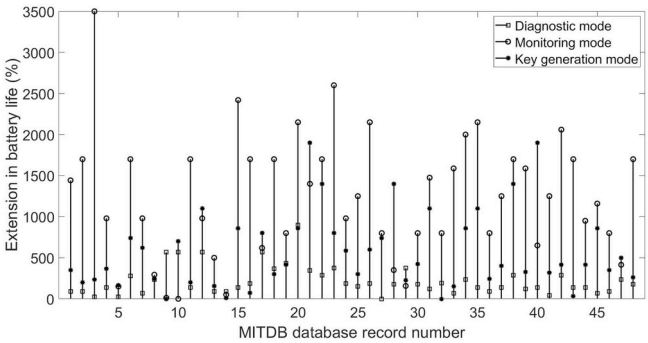

Fig. 13. Battery extension (%) of a sensor node considering its transmission cost in different modes for the entire MITDB database.

Table 12
Energy consumption of sensor nodes with tuned parameter values for MITDB records '103' (Record no. 4) and '234' (Record no. 48).

Mode of operation	Configurable	Record	$(N/M)_S$	$(Q)_s$	No. of bits transmitted	Battery (h)	Extension in battery life (%)
Diagnostic	No		3	10	2800	13.41	–
	Yes	103	4	8	1176	31.95	138
		234	8	7	1008	37.27	177
Monitoring	No		2	9	3780	9.94	–
	Yes	103	12	5	350	107.35	980
		234	24	6	210	178.92	1700
Key generation	No		2	12	5040	7.45	–
	Yes	103	7	9	1080	34.78	367
		234	3	5	1400	26.83	260

Table 13
Comparison of energy consumption at the gateway node between configurable and non-configurable system for MITDB record '100'.

	Task performed at the gateway node (Diagnostic mode)	Energy (J) for 1 day	
		Self-configurable N/M = 4, Q = 8	**Non-self-configurable N/M = 3, Q = 10**
1	Configuration of sensor nodes	**1.638**	–
2	Reception via XBee module	585.22	974.83
3	Feature extraction	141.65	159.44
4	128-bit biometric key generation	17.85	20.16
	Total	**746.358**	**1154.43**
	Battery lifetime (days)	**52**	**33.63**

non-configurable scenario. Table 12 shows the energy consumption of sensor nodes with tuned parameter values ($(N/M)_S$ and $(Q)_S$) for MITDB records '103' and '234', which are record numbers 4 and 48 respectively in Fig. 13.

As mentioned in Ref. [35], the energy consumption at the gateway node is largely due to the WiFi usage rather than any other signal processing tasks. The scenario used for energy profiling at the gateway node (Table 13) is as follows: (i) Configuring different modes: Initially the configuration modes are run at the gateway node in a plug and play scenario to determine the extent to which compression and bit-level quantization can be effectively brought into play at the connected sensor nodes, (ii) Monitoring ECG signal: By default, monitoring mode is activated to analyze the ECG data, and only during an emergency situation or end user request, diagnostic mode is activated to analyze and transmit ECG data to the cloud, and (iii) Cryptographic key generation: 128-bit key is generated periodically (in each minute) for authentication as well as for key management [30] between the gateway node and the sensor nodes connected to it. From Table 13, it is evident that the configuration task requires only very small amount of energy compared to other tasks. Also, we validated that the proposed self configurable gateway node enhances the battery lifetime of the gateway node when compared to the non-self-configurable case.

4. Discussion

In this paper, we used DBBD based CS encoding to achieve a plug and play design using N/M knob and quantization knob at the gateway node. To the best of our knowledge, there is no work available in the literature that addresses the real-time plug and play self-configurability of a WBAN based healthcare system. The self-configurability feature of our proposed system is mainly attributed to the DBBD matrix as discussed in section 2.2.2. The fine-tuning of compression parameter for DBBD based CS is solved by setting the N value as a highly composite number 840 or its multiples. We perform feature extraction directly from the compressed measurements using CS-SCGN. Performance evaluation for updating parameters at the gateway node without reconstructing the received CS measurements from the sensor node effectively reduces the computational and structural complexity of the system.

We addressed the self-configurability in ECG remote health monitoring by visualizing three modes of configuration. The optimization of communication cost can be achieved by means of these modes of configuration as illustrated in Fig. 11. The CS recovery stage in the performance evaluator of CS-SCGN is employed only for configuring the diagnostic mode. As exhibited in Table 10, the simplified CS recovery algorithm of [41] is faster and energy efficient. Thus, the proposed system provides desired QoS with the efficient utilization of available resources at the sensor node. The hardware implementation of self-configurable gateway node demonstrates that the various signal processing tasks performed will not load the resources available at the gateway node. In turn, it will increase the battery lifetime of sensor node (Fig. 11 and Table 12) as well as the gateway node (Table 13). We also successfully verified the proposed self-reconfigurable algorithm on datasets other than MITDB database.

5. Conclusion

In this paper, the design, implementation, and analysis of an efficient self-configurable IoT gateway node for ECG telemonitoring has been presented which can tune the compression and quantization parameters in three modes of configuration. This approach optimizes the energy efficiency of system by adaptively tuning the parameters to suit the signal dynamics as well as reconstruction quality requirements. CS using DBBD matrix is found to be very promising in accomplishing the self-configurability without compromising the resource constraint requirement of WBAN. The simulation as well as the hardware implementation results confirm the feasibility of the proposed system in ECG telemonitoring. Our proposed self-reconfigurable algorithm at the gateway node readily increased the battery lifetime of resource constrained sensor nodes by many folds without burdening the gateway node. This work can be extended to other ECG related physiological signals such as PPG and blood pressure, backed by corresponding performance parameters and evaluators in a WBAN based healthcare environment.

References

[1] T. Wu, F. Wu, J. Redout, M.R. Yuce, An autonomous wireless body area network implementation towards IoT connected healthcare applications, IEEE Access 5 (2017) 11413–11422.
[2] S.M.R. Islam, D. Kwak, M.H. Kabir, M. Hossain, K. Kwak, The Internet of Things for health care: a comprehensive survey, IEEE Access 3 (2015) 678–708.
[3] U. Satija, B. Ramkumar, M. Sabarimalai Manikandan, Real-time signal quality-aware ECG telemetry system for IoT-based health care monitoring, IEEE Internet Things J. 4 (3) (2017) 815–823.
[4] S. Movassaghi, M. Abolhasan, J. Lipman, D. Smith, A. Jamalipour, Wireless body area networks: a survey, IEEE Commun. Surveys Tuts. 16 (2014) 1658–1686.
[5] A. Pantelopoulos, N.G. Bourbakis, A survey on wearable sensor based systems for health monitoring and prognosis, IEEE Trans. Syst. Man Cybern. C Appl. Rev. 40 (2010) 1–12.

[6] Yusuf Salim, Srinath Reddy, Stephanie Ounpuu, Sonia Anand, Global burden of cardiovascular diseases, Circulation 104 (2001) 2855–2864.
[7] T. Tinnakornsrisuphap, R.E. Billo, An interoperable system for automated diagnosis of cardiac abnormalities from electrocardiogram data, IEEE J. Biomed. Health Inform. 19 (2) (2015) 493–500.
[8] Y. Zhang, Y. Zheng, W. Lin, H. Zhang, X. Zhou, Challenges and opportunities in cardiovascular health informatics, IEEE Trans. Biomed. Eng. 60 (3) (2013) 633–642.
[9] Sidharth Maheshwari, Acharyya Amit, Michele Schiariti, Paolo Emilio Puddu, Frank vectorcardiographic system from standard 12 lead ECG: an effort to enhance cardiovascular diagnosis, J. Electrocardiol. 49 (2) (2016) 231–242.
[10] S. Maheshwari, A. Acharyya, P. Rajalakshmi, P.E. Puddu, M. Schiariti, Accurate and reliable 3-lead to 12-lead ECG reconstruction methodology for remote health monitoring applications, Innov. Res. Biomed. Eng. 35 (2014) 341–350.
[11] L.N. Sharma, S. Dandapat, A. Mahanta, Multichannel ECG data compression based on multiscale principal component analysis, IEEE Trans. Inf. Technol. Biomed. 16 (2012) 730–736.
[12] A. Singh, L.N. Sharma, S. Dandapat, Multi-channel ECG data compression using compressed sensing in eigenspace, Comput. Biol. Med. 73 (2016) 24–37.
[13] Sibasankar Padhy, L.N. Sharma, S. Dandapat, Multilead ECG data compression using SVD in multiresolution domain, Biomed, Signal Process. Control 23 (2016) 10–18.
[14] R.J. Noble, J.S. Hillis, D.A. Rothbaum, Electrocardiography, H.K. Walker, W.D. Hall, J.W. Hurst (Eds.), Clinical Methods: the History, Physical, and Laboratory Examinations, third ed., Butterworths, Boston, 1990, pp. 164–185.
[15] M. Deng, C. Wang, M. Tang, T. Zheng, Extracting cardiac dynamics within ECG signal for human identification and cardiovascular diseases classification, Neural Netw. 100 (2018) 7083.
[16] S. Kesavan, G.K. Kalambettu, IoT enabled comprehensive, plug and play gateway framework for smart health, Proc. 2018 2nd Int. Conf. Adv. Electron. Comput. Commun. ICAECC, 2018, pp. 1–5.
[17] Daniele Bortolotti, Bojan Milosevic, Andrea Bartolini, Elisabetta Farella, Luca Benini, Quantifying the benefits of compressed sensing on a WBSN-based real-time biosignal monitor, Proc. Conf. Design, Automation & Test in Europe, 2016, pp. 732–737.
[18] A. Wang, F. Lin, Z. Jin, W. Xu, A configurable energy-efficient compressed sensing architecture with its application on body sensor networks, IEEE Trans. Ind. Informat. 12 (2016) 15–27.
[19] D.L. Donoho, Compressed sensing, IEEE Trans. Inf. Theory 52 (2006) 1289–1306.
[20] E.J. Candes, M.B. Wakin, An introduction to compressive sampling, IEEE Signal Process. Mag. 25 (2008) 21–30.
[21] D. Craven, B. McGinley, L. Kilmartin, M. Glavin, E. Jones, Energy-efficient compressed sensing for ambulatory ECG monitoring, Comput. Biol. Med. 71 (2016) 1–13.
[22] P. Charalampidis, Alexandros G. Fragkiadakis, Elias Z. Tragos, Rate-adaptive compressive sensing for IoT applications, Proc. IEEE 81st Vehicular Technology Conference, VTC Spring, 2015, pp. 1–5.
[23] V. Natarajan, A. Vyas, Power efficient compressive sensing for continuous monitoring of ECG and PPG in a wearable system, Proc. IEEE 3rd World Forum on Internet of Things, WF-IoT, 2016, pp. 336–341.
[24] A. Wang, F. Lin, Z. Jin, W. Xu, Ultra-low power dynamic knob in adaptive compressed sensing towards biosignal dynamics, IEEE Trans. Biomed. Circuits Syst. 10 (2016) 579–592.
[25] A.M. Rahmani, T.N. Gia, B. Negash, A. Anzanpour, I. Azimi, M. Jiang, P. Liljeberg, Exploiting smart e-Health gateways at the edge of healthcare Internet of Things: a Fog Computing approach, Future Gener. Comput. Syst. 78 (2018) 641–658.
[26] Eduard Marin, Argones Ra Enrique, Singele Dave, Bart Preneel, A Survey on Physiological-Signal-Based Security for Medical Devices, IACR Cryptology ePrint Archive, 2016.
[27] S. Bao, C.C.Y. Poon, Y. Zhang, L. Shen, Using the timing information of heartbeats as an entity identifier to secure body sensor network, IEEE Trans. Inf. Technol. Biomed. 12 (2008) 772–779.
[28] G. Zhang, C.C.Y. Poon, Y. Zhang, Analysis of using inter-pulse intervals to generate 128-bit biometric random binary sequences for securing wireless body sensor networks, IEEE Trans. Inf. Technol. Biomed. 16 (2012) 176–182.
[29] G. Zheng, G. Fang, R. Shankaran, M.A. Orgun, J. Zhou, L. Qiao, K. Saleem, Multiple ECG fiducial points based random binary sequence generation for securing wireless body area networks, IEEE J. Biomed. Health Inform. 21 (2017) 655–663.
[30] M. Aneesh, Koya, P.P. Deepthi, Anonymous hybrid mutual authentication and key agreement scheme for wireless body area network, Comput. Network. 40 (2018) 138–151.
[31] M. Davenport, M. Duarte, M. Wakin, D. Takhar, K. Kelly, R. Baraniuk, The smashed filter for compressive classification and target recognition, Proc. SPIE, 2007 January.
[32] M. Shoaib, N.K. Jha, N. Verma, Signal processing with direct computations on compressively sensed data, IEEE Trans. Very Large Scale Integr. Syst. 23 (2015) 30–43.
[33] D. Bortolotti, A. Bartolini, M. Mangia, R. Rovatti, G. Setti, L. Benini, Energy-aware bio-signal compressed sensing reconstruction: FOCUSS on the WBSN-gateway, Proc. 2015 IEEE 9th Int. Symposium on Embedded Multicore/Many-core Systems-On-Chip, 2015, pp. 120–126.
[34] D. Bortolotti, M. Mangia, A. Bartolini, R. Rovatti, G. Setti, L. Benini, Energy-aware bio-signal compressed sensing reconstruction on the WBSN-gateway, IEEE Trans. Emerg. Topics Comput. 6 (2018) 370–381.
[35] M. Al Disi, H. Djelouat, C. Kotroni, E. Politis, A. Amira, F. Bensaali, G. Dimitrakopoulos, G. Alinier, ECG signal reconstruction on the IoT-gateway and efficacy of compressive sensing under real-time constraints, IEEE Access 6 (2018) 69130–69140.
[36] ODROID-Hardkernel, http://www.hardkernel.com, (2019) accessed Jan 2019.
[37] D. Bortolotti, M. Mangia, A. Bartolini, R. Rovatti, G. Setti, L. Benini, An ultra-low power dual-mode ECG monitor for healthcare and wellness, Proc. 2015 Design, Automation & Test in Europe Conference & Exhibition (DATE), 2015, pp. 1611–1616 Grenoble.
[38] S. Qaisar, R.M. Bilal, W. Iqbal, M. Naureen, S. Lee, Compressive sensing: from theory to applications, a survey, J. Commun. Netw. 15 (5) (2013) 443–456.
[39] H. Mamaghanian, N. Khaled, D. Atienza, P. Vandergheynst, Compressed sensing for real-time energy-efficient ECG compression on wireless body sensor nodes, IEEE Trans. Biomed. Eng. 58 (9) (2011) 2456–2466.
[40] Z. He, T. Ogawa, M. Haseyama, The simplest measurement matrix for compressed sensing of natural images, Proc. 17th IEEE Int. Conf. Image Processing, ICIP), 2010, pp. 4301–4304.
[41] A. Ravelomanantsoa, H. Rabah, A. Rouane, Compressed sensing: a simple deterministic measurement matrix and a fast recovery algorithm, IEEE Trans. Instrum. Meas. 64 (12) (2015) 3405–3413.
[42] Y. Zigel, A. Cohen, A. Katz, The weighted diagnostic distortion(WDD) measure for ECG signal compression, IEEE Trans. Biomed. Eng. 47 (2000) 1422–1430.
[43] R.E. Blahut, Fast Algorithms for Digital Signal Processing, Addison-Wesley Publishing Company, Reading, MA, 1985.
[44] Bi Guoan, Yonghong Zeng, Transforms and Fast Algorithms for Signal Analysis and Representations, Springer Science & Business Media, 2003.
[45] S. Ramanujan, Highly composite numbers, Proc. London Math. Soc. Series 2 (14) (1915) 347–409.
[46] J. Pan, W. Tompkins, A real-time QRS detection algorithm, IEEE Trans. Biomed. Eng. 32 (1985) 230–236.
[47] A.L. Goldberger, L.A. Amaral, L. Glass, J.M. Hausdorff, P.C. Ivanov, R.G. Mark, J.E. Mietus, G.B. Moody, C.K. Peng, H.E. Stanley, PhysioBank, PhysioToolkit, and PhysioNet: components of a new research resource for complex physiologic signals, Circulation 101 (23) (2000) e215–e220.
[48] A. Taddei, G. Distante, M. Emdin, P. Pisani, G.B. Moody, C. Zeelenberg, C. Marchesi, The European ST-T database: standard for evaluating systems for the analysis of ST-T changes in ambulatory electrocardiography, Eur. Heart J. 13 (1992) 1164–1172.
[49] J.A. Tropp, A.C. Gilbert, Signal recovery from random measurements via orthogonal matching pursuit, IEEE Trans. Inf. Theory 53 (2007) 4655–4666.
[50] XCTU, https://www.digi.com/products/iot-platform/xctu, (2019) accessed Feb. 2019.
[51] L.H. Wang, T.Y. Chen, K.H. Lin, Q. Fang, S.Y. Lee, Implementation of a wireless ECG acquisition SoC for IEEE 802.15.4 (ZigBee) applications, IEEE J. Biomed. Health Informat. 19 (1) (2015) 247–255.

Aneesh M. Koya received B. Tech. degree in Electronics and Communication Engineering from M.E.S. College of Engineering, Malappuram (University of Calicut) in 2008 and M. Tech. degree in Communication Engineering from N. S. S. College of Engineering, Palakkad (University of Calicut) in 2013. He is currently working toward the Ph.D. degree in Electronics and Communication Engineering from National Institute of Technology Calicut. His research interests include wireless body area network, cryptography and signal processing.

Deepthi P. P. received B. Tech. degree in Electronics and Communication Engineering from N. S. S. College of Engineering, Palakkad (University of Calicut) in 1991, M. Tech. Degree in Instrumentation from Indian Institute of Science, Bangalore in 1997 and Ph.D. from National Institute of Technology Calicut in the field of Secure Communication in 2009. She has been working as Faculty in institutions under IHRD, Thiruvananthapuram from 1992 to 2001 and in the Department of Electronics & Communication Engineering, National Institute of Technology Calicut from 2001 onwards. Her current interests include signal processing with security applications, cryptographic system implementations, information theory and coding theory.